Polymerization Catalysts

DOI: 10.1002/ange.200600666

Endowing Aspecific, Unbridged-Metallocene Propylene-Polymerization Catalysts with Isospecificity: The Unprecedented Role of MAO**

*Seong Kyun Kim, Hwa Kyu Kim, Min Hyung Lee, Seung Woong Yoon, and Youngkyu Do**

The relationship between the nature of catalyst systems and the resulting polymer has been well established in single-site olefin-polymerization systems and now provides the opportunity to tailor the polymer's properties.[1–4] In particular, chiral *ansa*-metallocene catalysts, which follow an enantiomorphic site-control mechanism, have been intensively investigated to obtain stereochemical control of propylene polymerization by varying the ligand structure.[5–7] Unbridged-metallocene-based systems, on the other hand, have received little attention owing to their aspecific nature[8,9] in spite of their ability to produce iso-rich[10,11] or isotactic–atactic block polypropylene[12,13] when containing rotationally hindered ligands. As unbridged metallocenes are far easier to synthesize than *ansa*-metallocenes, we have been investigating isospecific, unbridged-metallocene catalytic systems that can be generated in situ during the activation step. To this end, we have designed "class I" unbridged metallocenes, a new class analogous to the known aspecific, unbridged metallocenes of "class II".[8,9] The Lewis basic sites E in class I complexes are found to interact with $[\text{Me-MAO}]^-$ to generate rigid, *rac*-like cationic active species, thereby endowing aspecific, unbridged-metallocene precatalysts with isospecificity. Herein, we report a novel example of a sterically unhindered, unbridged zirconocene system that is able to produce highly isotactic polypropylene through the unprecedented role of methyl aluminum oxane (MAO).

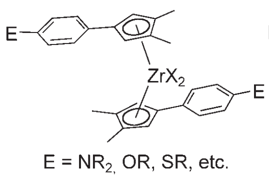

class I

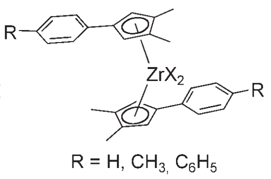

class II

The amine-functionalized, unbridged zirconocenes $[\{1\text{-}(p\text{-}Me_2NC_6H_4)\text{-}3,4\text{-}Me_2C_5H_2\}_2ZrX_2]$ $[(AP)_2ZrX_2$; X = Cl (**2**), X = Me (**3**)] were obtained from newly synthesized ligand **1** as outlined in Scheme 1. The molecular structure of **2** has C_2 symmetry in the solid state (Figure 1). The polymerization of propylene with **2**/MAO ([Al]/[Zr] = 1000) was performed at various temperatures (T_p = 0, 25, 50, and 70 °C; Table 1, entries 1–4, respectively). The **2**/MAO system shows lower catalytic activity but produces higher molecular weight polypropylenes than the well-known isospecific catalyst *rac*-$[Et(Ind)_2ZrCl_2]$ (EBIZr)/MAO (entry 9) under identical reaction conditions. The differential scanning calorimetry (DSC) and gel permeation chromatography (GPC) traces indicate that all the crude polypropylenes from the **2**/MAO system show multiple melting transitions (T_m) and broad molecular-weight distributions (M_w/M_n) of between 4.5 and 11 (Figure 2).

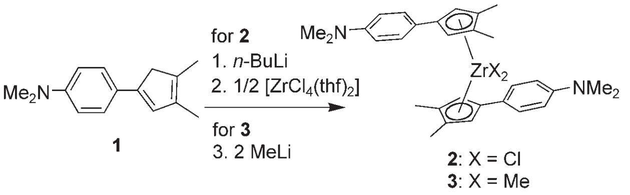

Scheme 1. Synthetic routes to zirconocenes **2** and **3**.

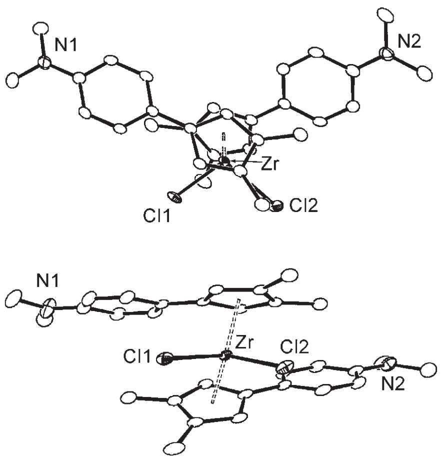

Figure 1. Molecular structure of **2**. Top: top view; bottom: side view.

The crude polypropylenes were fractionated by stepwise solvent extraction[14] into three portions for further analysis, 1) diethyl ether soluble, 2) diethyl ether insoluble and *n*-heptane soluble, and 3) diethyl ether insoluble and *n*-heptane insoluble. The *mmmm* methyl pentad values in Table 2 suggest that these portions correspond to atactic-like, mod-

---

[*] Dr. S. K. Kim, H. K. Kim, Dr. M. H. Lee, S. W. Yoon, Prof. Dr. Y. Do
Department of Chemistry
School of Molecular Science BK-21
Center for Molecular Design and Synthesis
and
Polyolefin Materials Research Center
Korea Advanced Institute of Science and Technology
Daejeon, 305-701 (Republic of Korea)
Fax: (+82) 42-869-2810
E-mail: ykdo@kaist.ac.kr
Homepage: http://xray.kaist.ac.kr/

[**] The authors are grateful for financial support from CMDS, POMRC, the BK-21 project, and the Honam Petrochemical Co. S.K.K. thanks Mr. H. S. Shin for performing the NMR spectroscopy experiments. MAO = methyl aluminum oxane.

Supporting Information for this article is available on the WWW under http://www.angewandte.org or from the author.

Table 1: Propylene polymerization data.[a]

Entry	Cat.	Cocat.	T_p [°C]	Yield [g]	Act.[b]	M_w [$\times10^{-3}$]	$M_\mathrm{w}/M_\mathrm{n}$
1	**2**	MAO	0	1.02	102	227	4.56
2	**2**	MAO	25	6.24	624	166	10.7
3	**2**	MAO	50	7.25	725	32.0	9.50
4	**2**	MAO	70	3.41	341	10.1	5.27
5	**3**	MAO	25	6.38	638	168	11.4
6[c]	**3**	borate/TIBA	25	6.95	695	15.2	2.10
7[c]	**3**	borate/TOA	25	2.37	237	16.6	2.10
8[d]	BPZr	MAO	0	2.83	566	58.9	1.87
9[e]	EBIZr	MAO	25	12.4	5930	19.1	2.13
10[f]	**3**	MAO	25	1.02	204	126	12.4
11[f]	**3**	MAO/borate	25	2.18	435	13.3	2.66
12[f]	**3**	borate/MAO	25	1.22	244	22.4	2.00

[a] Polymerization conditions: P(propylene) = 1 bar, [Zr] = 5.0 μmol, [Al]/[Zr] = 1000, solvent = 50 mL of toluene, t_p = 120 min; Entry numbers 1–9 correspond to those in Table 2. [b] Activity, in units of (kg of PP)/[(mol of Zr) h bar]. [c] borate = $[Ph_3C][B(C_6F_5)_4]$; TIBA = triisobutylaluminum; TOA = trioctylaluminum; [B]/[Zr] = 1, [Al]/[Zr] = 200. [d] t_p = 60 min; BPZr = $[\{1\text{-}(p\text{-}C_6H_5C_6H_4)\text{-}3,4\text{-}Me_2C_5H_2\}_2ZrCl_2]$. [e] t_p = 25 min; EBIZr = *rac*-$[Et(Ind)_2ZrCl_2]$. [f] t_p = 60 min; [Al]/[Zr] = 200, [B]/[Zr] = 1.

erately isotactic, and highly isotactic polypropylenes, respectively. The amount of *n*-heptane insoluble polypropylene decreases as the polymerization temperature increases, while that of the diethyl ether soluble portion increases. The *n*-heptane insoluble portions have remarkably high *mmmm* values of around 86% (Figure 3A) and a T_m of 151 °C (Table 2, entry 2). The class II complex $[\{1\text{-}(p\text{-}C_6H_5C_6H_4)\text{-}3,4\text{-}Me_2C_5H_2\}_2ZrCl_2]$ (BPZr)[9] gives atactic polypropylene even at 0 °C (entry 8). These results clearly demonstrate that the unbridged zirconocene **2**/MAO system is capable of producing highly isotactic polypropylene and also that the simple functionalization of class II to class I metallocenes should be an effective route for endowing aspecific, unbridged-metallocene precatalysts with isospecificity.

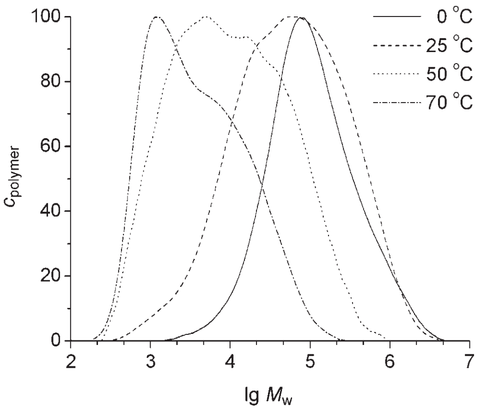

Figure 2. Molecular-weight distribution of the polymers obtained with **2**/MAO.

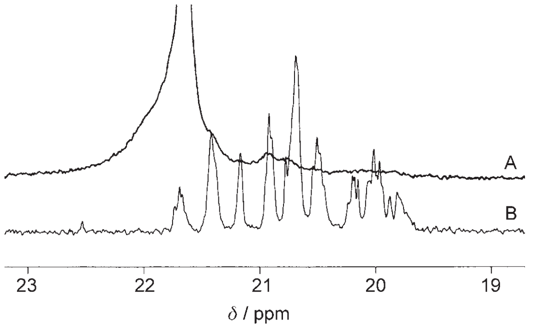

Figure 3. Methyl region of the ^{13}C NMR spectra of polypropylenes obtained from the *n*-heptane insoluble portion from: A) the reaction with **2**/MAO given as entry 2 of Table 1 and Table 2 and B) for the crude polymer obtained from the reaction with **3**/borate/TIBA given as entry 6 of Table 1 and Table 2.

Table 2: Detailed analysis of each extracted portion of the polymer samples.[a]

Entry[b]	Extraction portion	Wt %	T_m [°C]	M_w [$\times10^{-3}$]	$M_\mathrm{w}/M_\mathrm{n}$	*mmmm* [%]
1	EE-sol	13	–	n/d[c]	n/d[c]	14
	EE-insol/C7-sol	21	151.1	85.8	2.45	55
	C7-insol	66	155.7	337	3.44	85
2	EE-sol	20	–	27.2	5.23	19
	EE-insol/C7-sol	21	131.8	68.4	4.20	53
	C7-insol	59	151.3	273	4.26	86
3	EE-sol	50	–	10.7	4.66	17
	EE-insol/C7-sol	32	146.4	39.4	3.80	67
	C7-insol	18	148.3	113	2.59	86
4	EE-sol	64	–	5.3	3.35	19
	EE-insol/C7-sol	22	127.3	17.8	2.59	53
	C7-insol	14	140.6	48.1	2.18	86
5	EE-sol	21	n/d[c]	n/d[c]	n/d[c]	n/d[c]
	EE-insol/C7-sol	44	n/d[c]	n/d[c]	n/d[c]	n/d[c]
	C7-insol	35	n/d[c]	n/d[c]	n/d[c]	n/d[c]
6	EE-sol	100	–	15.2	2.10	5.4
7	EE-sol	100	–	16.6	2.10	3.2
8	EE-sol	100	–	58.9	1.87	n/d[c]
9	EE-insol/C7-sol	97	129	19.1	2.13	76

[a] EE = diethyl ether, C7 = *n*-heptane; See Supporting Information for detailed analysis. [b] Entry numbers correspond to those in Table 1. [c] Not determined.

The use of **3**, the dimethyl analogue of **2**, provides clues to the nature of the isospecific catalytic species in the **2**/MAO system. When **3** is activated with $[Ph_3C][B(C_6F_5)_4]$ in the presence of TIBA or TOA ([Al]/[Zr] = 200),[15] for example, the resulting catalytic systems give completely diethyl ether soluble, atactic polypropylenes (Figure 3B; see also Tables 1 and 2 entries 6 and 7), while **3**/MAO affords polypropylene whose tacticity distribution is similar to that obtained with **2**/MAO (see Tables 1 and 2, entry 5). Therefore, the involvement of MAO appears to be essential in achieving isospecificity in propylene polymerization. Furthermore, when the activation of **3** is effected by initial treatment with MAO and subsequent treatment with $[Ph_3C][B(C_6F_5)_4]$ (see Table 1, entry 11), the resulting catalytic species gives completely atactic, diethyl ether soluble polypropylene whose M_w/M_n value of 2.66 reflects its single-site catalytic nature. ^{1}H NMR spectroscopy experiments revealed that the addition of $[Ph_3C][B(C_6F_5)_4]$ to **3**/MAO causes the formation of Ph_3CMe, as judged by the appearance of a signal at $\delta = 1.96$ ppm,[16] while the treatment of neutral MAO with $[Ph_3C][B(C_6F_5)_4]$ at room temperature does not produce Ph_3CMe. Since $[Me\text{-}MAO]^-$ is the generally assumed counteranion formed in metallocene/MAO systems,[17] the formation of Ph_3CMe can be understood in terms of Me^- abstraction by $[Ph_3C]^+$ from $[Me\text{-}MAO]^-$.[18] Therefore, the treatment of **3**/MAO with $[Ph_3C][B(C_6F_5)_4]$ causes the transformation of the isospecific $[(AP)_2ZrMe]^+$-$[Me\text{-}MAO]^-$ in **3**/MAO to aspecific $[(AP)_2ZrMe]^+[B(C_6F_5)_4]^-$ and neutral MAO. This observation, and the additional finding that the catalytic system generated by treating **3** initially with $[Ph_3C][B(C_6F_5)_4]$ ($[B]/[Zr] = 1$) and then with MAO ($Al/Zr = 200$) (see Table , entry 12) also gives completely atactic polypropylene, implies that the influence of MAO on the isospecificity occurs due to $[Me\text{-}MAO]^-$ rather than neutral MAO.

Variable-temperature ^{1}H NMR spectroscopy studies of **3** and **3**/MAO ($Al/Zr = 200$) solutions in $[D_8]$toluene (Figure 4)[16] provide further evidence for the nature of the isospecific catalytic species. The singlet appearance of the two magnetically different Cp protons of **3** at temperatures as low as 203 K suggests that the ligand in **3** rotates rapidly in solution. Waymouth-type neutral precatalysts undergo very rapid ligand rotation in solution,[19] and the bulky precatalyst bis(2-(3,5-di-*tert*-butylphenyl)indenyl)dimethylzirconium rotates at a rate of 94 700 s^{-1} even at 196 K, as measured by the longitudinal relaxation time.[20] Therefore, the ligand rotation rate of compound **3** should be at least of the order of 10^4 s^{-1} at the low-temperature limit.

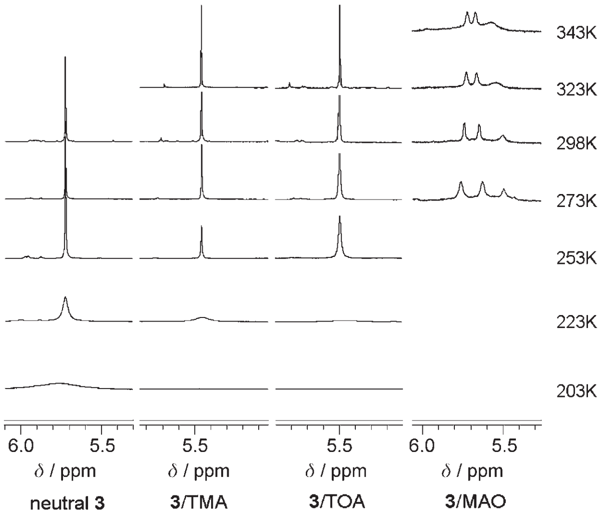

Figure 4. Cyclopentadienyl (Cp) proton region of the variable-temperature NMR (VT-NMR) spectra of **3**, **3**/TMA, **3**/TOA(Al/Zr=3), and **3**/MAO(Al/Zr=200). TMA = trimethylaluminum.

The addition of MAO to **3** causes the appearance of one set of two Cp proton signals, with equal intensities, at around $\delta = 5.7$ ppm and an upfield shift of the Me_2N signal,[21] thus indicating the presence of an active species in which the ligand rotation is restricted on the NMR timescale, up to 343 K, and the formation of Al···N interactions, respectively. Although coalescence was not observed up to 343 K, the ligand rotation rate of the active species in **3**/MAO can be calculated as 122 s^{-1} at the coalescence temperature by taking 273 K as the no-exchange limit;[22] it is therefore slower than 122 s^{-1} at the polymerization temperatures.

The position of the upfield-shifted Me_2N signal shows a large temperature dependency such that at the higher temperature limit the chemical-shift value approaches that of neutral **3**. Therefore, the Al···N Lewis acid–base interaction is stable at the low-temperature limit but is likely to be cleaved at the higher temperature limit, thereby leading to a thermal equilibrium between the species with and without this interaction. **3**/TMA and **3**/TOA ($Al/Zr = 3$) systems also show an upfield shift of the Me_2N signal but only one Cp proton signal. Thus, trialkylaluminum is capable of forming an Al···N interaction but is not able to prevent the ligand rotation.

Overall, the above observations support the formation of a *rac*-like ion-pair of the type $[(AP)_2ZrP]^+[Me\text{-}MAO]^-$ (**IS**) as the isospecific catalytic species (Scheme 2). The simultaneous presence of the cation–anion pairing and interactions between the Lewis acid sites in $[Me\text{-}MAO]^-$ and the nitrogen atoms of the amine-functionalized, unbridged-zirconocene cation in **IS** is effective in preventing the ligands from rotating rapidly, which leads to the prevalence of a racemic, C_2-symmetric-like active species in solution. The fact that the hydrodynamic diameter (25 Å)[23] of $[Me\text{-}MAO]^-$ is larger than the separation (ca. 15 Å) between two nitrogen atoms in **2** is also in favor of such interactions. The broad molecular-weight distribution as well as the presence of polymer fractions with different tacticities associated with **2**/MAO imply that **IS** is in thermal equilibrium with the other species shown in the upper part of Scheme 2. A similar temperature-dependent Al···N interaction has been employed in alkylamine-functionalized zirconocene/MAO to modulate the molecular-weight distribution of polyethylene.[24] Clearly,

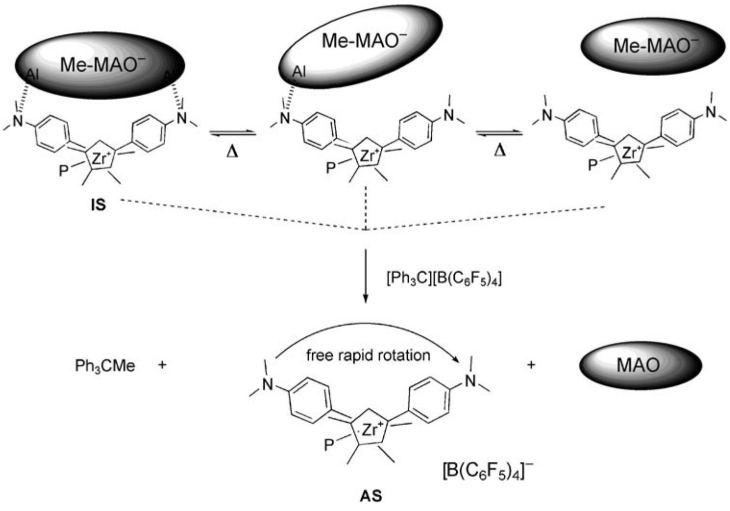

Scheme 2. Suggested thermal equilibrium of possible active species upon MAO activation (top) and generation of the aspecific active species **AS** by the addition of $[Ph_3C][B(C_6F_5)_4]$ to the **3**/MAO system (bottom).

MAO, in the form of $[\text{Me-MAO}]^-$, acts as an in situ *ansa*-bridge and plays the unprecedented role of endowing aspecific class I unbridged-metallocene precatalysts with isospecificity, although cocatalysts are also known to affect the stereoselectivity of unbridged-metallocene catalysts to some extent.[25–27]

In conclusion, we have devised a novel synthetic strategy for the synthesis of isospecific, unbridged-metallocene catalytic systems for propylene polymerization. The class I unbridged metallocene with $E = NEt_2$, OMe, SMe, etc. behaves similarly and efforts are continuing to establish the scope of the synthetic strategy.[28]

Received: February 20, 2006
Revised: June 9, 2006

Keywords: isotactic polypropylene · Lewis acids · metallocenes · polymerization · zirconium

---

[1] Special issue on *Frontiers in Metal-Catalyzed Polymerization* (Ed.: J. A. Gladysz): *Chem. Rev.* **2000**, *100*, 1167.
[2] V. C. Gibson, S. K. Spitzmesser, *Chem. Rev.* **2003**, *103*, 283.
[3] W. Kaminsky, *Adv. Catal.* **2001**, *46*, 89.
[4] H. H. Brintzinger, D. Fischer, R. Mülhaupt, B. Rieger, R. M. Waymouth, *Angew. Chem.* **1995**, *107*, 1255; *Angew. Chem. Int. Ed. Engl.* **1995**, *34*, 1143.
[5] L. Resconi, L. Cavallo, A. Fait, F. Piemontesi, *Chem. Rev.* **2000**, *100*, 1253.
[6] J. A. Ewen, M. J. Elder, R. L. Jones, A. L. Rheingold, L. M. Liable-Sands, R. D. Sommer, *J. Am. Chem. Soc.* **2001**, *123*, 4763.
[7] S. A. Miller, J. E. Bercaw, *Organometallics* **2004**, *23*, 1777.
[8] J. L. Maciejewski Petoff, M. D. Bruce, R. M. Waymouth, A. Masood, T. K. Lal, R. W. Quan, S. J. Behrend, *Organometallics* **2004**, *23*, 1777.
[9] M. H. Lee, Y. Do, *J. Organomet. Chem.* **2005**, *690*, 1240.
[10] G. Erker, R. Nolte, R. Aul, S. Wilker, C. Krüger, R. Noe, *J. Am. Chem. Soc.* **1991**, *113*, 7594.
[11] A. Razavi, *J. Am. Chem. Soc.* **1993**, *115*, 7529.
[12] G. Coates, R. M. Waymouth, *Science* **1995**, *267*, 217.
[13] S. Lin, R. M. Waymouth, *Acc. Chem. Res.* **2002**, *35*, 765.
[14] A. Lehtinen, R. Paukkeri, *Macromol. Chem. Phys.* **1994**, *195*, 1539.
[15] The use of additional AlR_3 is required since the treatment of **3** with $[Ph_3C][B(C_6F_5)_4]$ did not afford active species. A similar phenomenon is also reported in ref. [24].
[16] See Supporting Information for more details.
[17] E. Y.-X. Chen, T. J. Marks, *Chem. Rev.* **2000**, *100*, 1391.
[18] The formation of Ph_3CMe from $[Ph_3C]^+$ by the abstraction of Me^- from the anionic dinuclear alumoxane has been reported: S. J. Obrey, S. G. Bott, A. R. Barron, *Organometallics* **2001**, *20*, 5162.
[19] M. D. Bruce, G. W. Coates, E. Hauptman, R. M. Waymouth, J. W. Ziller, *J. Am. Chem. Soc.* **1997**, *119*, 11174.
[20] G. M. Wilmes, M. B. France, S. R. Lynch, R. M. Waymouth, *Organometallics* **2004**, *23*, 2405.
[21] The intensity of the upfield peak at $\delta = 5.5$ ppm is dependent on the [Al]/[Zr] ratio. This peak disappears at ratios higher than 200. Its origin is considered to be due to a **3**···TMA species since a mixture of **3** and TMA gives a Cp signal at the same position.
[22] A $[D_8]$toluene solution of **3**/MAO at 273 K is extremely viscous and no proton signal was seen at the lower temperatures. Thus, 273 K was taken as the no-exchange limit. In addition, owing to the possible influence of viscosity on the line width at 273 K, the line-shape-analysis expression $(k = \pi((W_{1/2})_e - (W_{1/2})_o)$ where $W_{1/2}$, e, and o stand for the peak-width at half height, with exchange, and no exchange, respectively, for the rates in the slow-exchange regime below the coalescence point cannot be used. Thus, the rotation rate at the coalescence point was calculated and taken as a comparison value: $k = \pi \Delta \nu_0 / 2^{1/2} = \pi (2307–2252\ \text{Hz})/2^{1/2} = 122\ \text{s}^{-1}$.
[23] D. E. Babushkin, H. H. Brintzinger, *J. Am. Chem. Soc.* **2002**, *124*, 12869.
[24] C. Müller, D. Lilge, M. O. Kristen, P. Jutzi, *Angew. Chem.* **2000**, *112*, 800; *Angew. Chem. Int. Ed.* **2000**, *39*, 789.
[25] G. M. Wilmes, J. L. Polse, R. H. Waymouth, *Macromolecules* **2002**, *35*, 6766.
[26] V. Busico, V. V. A. Castelli, P. Aprea, R. Cipullo, A. Segre, G. Talarico, M. Vacatello, *J. Am. Chem. Soc.* **2003**, *125*, 5451.
[27] A. Macchioni, *Chem. Rev.* **2005**, *105*, 2039.
[28] CCDC 299059 contains the supplementary crystallographic data for this paper. These data can be obtained free of charge from The Cambridge Crystallographic Data Centre via www.ccdc.cam.ac.uk/data_request/cif.